



## Molecular Crystals and Liquid Crystals

Publication details, including instructions for authors and subscription information:

<http://www.tandfonline.com/loi/gmcl20>

### Structural and Magnetic Properties of Polypyrrole Nanocomposites

R. Turcu<sup>a</sup>, I. Peter<sup>a</sup>, O. Pana<sup>a</sup>, L. Giurgiu<sup>a</sup>, N. Aldea<sup>a</sup>, B. Barz<sup>a</sup>, M. N. Grecu<sup>b</sup> & A. Coldea<sup>c</sup>

<sup>a</sup> National Institute R&D Isotopic and Molecular Technologies, Romania

<sup>b</sup> National Institute of Materials Physics, Bucuresti-Magurele, Romania

<sup>c</sup> Clarendon Laboratory, Oxford University, Oxford, United Kingdom

Version of record first published: 18 Oct 2010

To cite this article: R. Turcu, I. Peter, O. Pana, L. Giurgiu, N. Aldea, B. Barz, M. N. Grecu & A. Coldea (2004): Structural and Magnetic Properties of Polypyrrole Nanocomposites, *Molecular Crystals and Liquid Crystals*, 417:1, 235-243

To link to this article: <http://dx.doi.org/10.1080/15421400490478939>

PLEASE SCROLL DOWN FOR ARTICLE

Full terms and conditions of use: <http://www.tandfonline.com/page/terms-and-conditions>

This article may be used for research, teaching, and private study purposes. Any substantial or systematic reproduction, redistribution, reselling, loan, sub-licensing, systematic supply, or distribution in any form to anyone is expressly forbidden.

The publisher does not give any warranty express or implied or make any representation that the contents will be complete or accurate or up to date. The accuracy of any instructions, formulae, and drug doses should be independently verified with primary sources. The publisher shall not be liable for any loss, actions, claims, proceedings, demand, or costs or damages whatsoever or howsoever caused arising directly or indirectly in connection with or arising out of the use of this material.

## STRUCTURAL AND MAGNETIC PROPERTIES OF POLYPYRROLE NANOCOMPOSITES

---

*R. Turcu, I. Peter, O. Pana, L. Giurgiu, N. Aldea, and B. Barz*  
*National Institute R&D Isotopic and Molecular Technologies,*  
*P.O. Box 700, 3400, Cluj-Napoca 5, Romania*

*M. N. Grecu*  
*National Institute of Materials Physics, P.O. Box MG-7*  
*Bucuresti-Magurele, Romania*

*A. Coldea*  
*Oxford University, Clarendon Laboratory, Parks Road,*  
*Oxford, United Kingdom*

*We report the synthesis and characterization of conducting polymer nanocomposites based on polypyrrole (PPY) and  $\text{Fe}_2\text{O}_3$  magnetic particles. The global structure of PPY nanocomposites was obtained by X-ray Diffraction (XRD) method using a new approximation based on Generalized Fermi Function. The local structural parameters of Fe sites in  $\text{Fe}_2\text{O}_3$  nanocrystallites embedded in PPY were determined by X-ray Absorption Spectroscopy (EXAFS). The lack of hysteresis loop for the magnetization curves of the composite PPY- $\text{Fe}_2\text{O}_3$  indicates a superparamagnetic behavior which is typical for nanosized magnetic particles.*

## INTRODUCTION

The inorganic-organic nanocomposites are a new class of advanced materials studied with growing interest over the last few years. The synthesis of nanocomposites containing organic conducting polypyrrole (PPY) and inorganic magnetic particles represents a new strategy to obtain the specific

The authors are grateful to Beijing Synchrotron Radiation Facilities (BSRF) for the beam time and to Hu Tiandou, Liu Tao, Xie Yaning, Ziyu Wu, Jing Zhang and Du Yonghua for their technical assistance in EXAFS and XRD measurements. This work was financially supported by the Romanian Ministry of Education and Research, project nr. 4/12.11.2002.

Address correspondence to R. Turcu, National Institute R&D Isotopic and Molecular Technologies, P.O. Box 700, Cluj-Napoca 5, 3400 Romania. E-mail: turcu@L30.itim-cj.ro

requirements of physical properties for different applications like electromagnetic interference shielding, microwave absorbing, chemical sensors [1–3].

In this paper we report the synthesis and characterization of the nanocomposites obtained by combining the organic conducting PPY with  $\text{Fe}_2\text{O}_3$  magnetic particles. The X-ray diffraction spectra demonstrate the formation of hematite  $\alpha\text{-Fe}_2\text{O}_3$  nanoparticles in PPY matrix. The lack of hysteresis loop for the PPY- $\text{Fe}_2\text{O}_3$  magnetization curve indicates a superparamagnetic behavior which is typical for nanosized magnetic particles.

## EXPERIMENTAL

### Samples Preparation

The host PPY matrix was prepared by in situ doping polymerization method. The dopant, 0.24 M dodecylsulfonic acid sodium salt (DSNa) and the monomer, 0.48 M pyrrole were dissolved in water under vigorous stirring at room temperature. An aqueous ammonium persulfat (APS) solution (0.096 M) was added slowly to the mixture. PPY doped with  $\text{DS}^-$  ions, obtained as a black powder, was poured into 1 M NaOH aqueous solution under stirring. During the reaction of polymer reduction, the  $\text{Na}^+$  cations are inserted into PPY matrix. Then, the reduced PPY was immersed into 1 M  $\text{FeCl}_3$  aqueous solution under stirring 24 h, to allow the exchange of  $\text{Na}^+$  cations by  $\text{Fe}^{3+}$  cations into the polymer. Hereafter, the composite obtained by this reaction is named 1PPY- $\text{Fe}_2\text{O}_3$ . During the cations exchange process, an oxidation reaction of the neutral PPY chains segments occurs due to the reduction of  $\text{Fe}^{3+}$  to  $\text{Fe}^{2+}$ . It results in a decrease of  $\text{Fe}^{3+}$  ions concentration in the solution. Hence, for some PPY samples, the initial  $\text{FeCl}_3$  solution was replaced after 12 h by a freshly prepared one containing the same concentration, 1 M  $\text{FeCl}_3$  and the reaction was continued for 12 h. The samples obtained in this way is named 2PPY- $\text{Fe}_2\text{O}_3$ . The treatment of PPY samples containing  $\text{Fe}^{3+}$  with 1 M  $\text{NH}_4\text{OH}$  aqueous solution at  $70^\circ\text{C}$  for 30 min results in the formation of  $\text{Fe}_2\text{O}_3$  nanoparticles into the PPY matrix.

### Measurements Methods

The crystalline phase of the samples was investigated by X-ray diffraction (XRD) with  $\text{CuK}\alpha$  radiation (0.1542 nm) on a RigaK D/MAX -  $\gamma$ A diffractometer (80 keV and 100 mA). The transmission EXAFS measurements were carried out in 4W1B beam lines at Beijing Synchrotron Radiation Facilities (BSRF) operating at 30–50 mA and 2.2 GeV at room temperature.

The spectra were recorded in the transmission mode by using X-ray in the energy range 6.91–7.88 keV. The hematite powder,  $\alpha\text{-Fe}_2\text{O}_3$  was used as a standard sample. The absorption coefficients of the Fe K edge were determined by using a Si (111) double crystal monochromator. The EXAFS analysis of absorption coefficients was done using the computer codes EXAFS31 to EXAFS36 [4] from our library and the CDXAS code [5].

FTIR transmission spectra of PPY nanocomposites powder embedded in KBr were recorded using a JASCO FTIR 610 spectrophotometer.

The magnetic properties of PPY- $\text{Fe}_2\text{O}_3$  nanocomposites were investigated using a SQUID device. The electron spin resonance (ESR) spectra of PPY- $\text{Fe}_2\text{O}_3$  samples were determined by a JEOL JES-ME-3X spectrometer.

## RESULTS AND DISCUSSIONS

The Figure 1 shows the XRD spectra of PPY- $\text{Fe}_2\text{O}_3$  nanocomposites. It is well known that PPY is an amorphous materials having an XRD spectrum with a broad maximum around  $2\theta = 20^\circ$  [6]. The nanocomposites PPY-

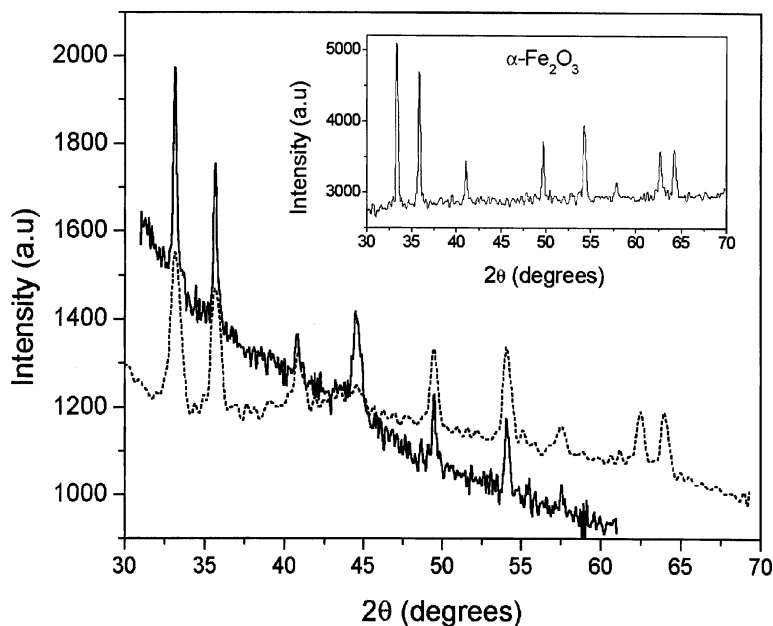


**FIGURE 1** The X-ray diffraction spectra for polypyrrole nanocomposites: 1PPY- $\text{Fe}_2\text{O}_3$  (full line); 2PPY- $\text{Fe}_2\text{O}_3$  (dotted line). Inset: the spectrum for the standard polycrystalline  $\alpha\text{-Fe}_2\text{O}_3$ .

$\text{Fe}_2\text{O}_3$  contain a crystalline phase ( $\text{Fe}_2\text{O}_3$  nanoparticle) embedded in the amorphous PPY matrix. The characteristic peaks of  $\alpha\text{-Fe}_2\text{O}_3$  (see the inset of Figure 1) can be clearly observed in the both spectra of the nanocomposites shown in the Figure 1. The global structure as described by the average particle size and the microstrain parameters was determined from XRD analysis. X-ray Lines Profile (XRLP) were approximated by the Generalized Fermi Function [7]. Taking into account the convolution product of the experimental and instrumental XRLP, the integral width  $\delta_f$  of the true sample can be express by the relation [7]

$$\delta_f(\rho_h, \rho_g) = \frac{\pi}{2\rho_h \cos \frac{\pi\rho_h}{2\rho_g}} \left( \cos \frac{\pi\rho_h}{\rho_g} + 1 \right) \quad (1)$$

where  $\rho_h, \rho_g$  are the half sum of the shape parameters for the experimental and instrumental profiles, respectively.

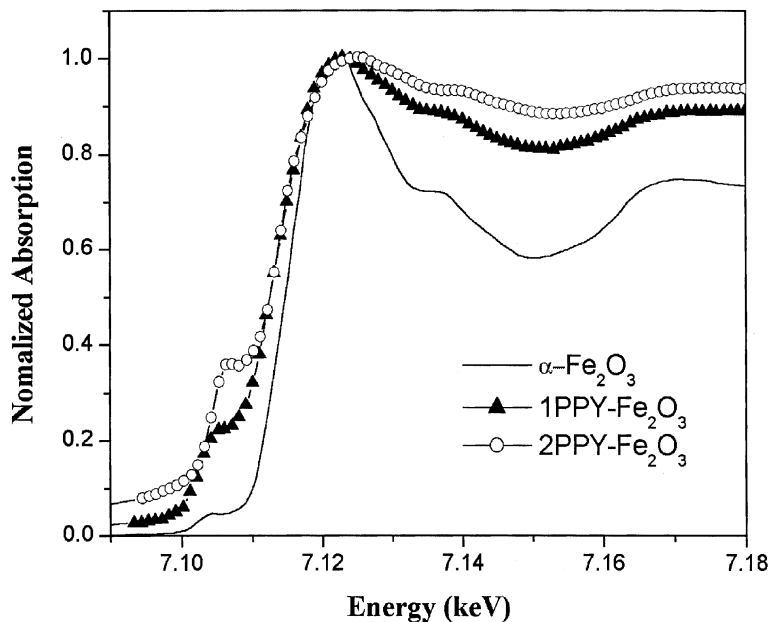
The investigated  $\alpha\text{-Fe}_2\text{O}_3$  has hexagonal symmetry. Therefore the following relation was used to calculate the average particle size [8]

$$\frac{\delta_f \cos \theta}{\lambda} = \frac{1}{D_{\text{eff}}} + \frac{\varepsilon \sin \theta}{\lambda} \quad (2)$$

where  $\theta$  is the Bragg angle of the profiles,  $\lambda$  is the X-ray wavelength,  $D_{\text{eff}}$  is the effective particle size and  $\varepsilon$  is the effective microstrain.

Different values of these structural parameters were obtained for the investigated nanocomposites:  $D_{\text{eff}} = 67.77 \text{ nm}$ ,  $\varepsilon = 1.7107 \times 10^{-6}$  and  $D_{\text{eff}} = 11.75 \text{ nm}$ ,  $\varepsilon = 3.987 \times 10^{-5}$  for 1PPY  $\text{Fe}_2\text{O}_3$  and 2PPY  $\text{Fe}_2\text{O}_3$ , respectively.

The Figure 2 shows the EXAFS spectra of the investigated samples. The extraction of the EXAFS signal is based on the determination of the binding energy,  $E_o$  for  $\text{Fe}^{3+}$  K-edge, followed by background removal by pre-edge and after-edge fitting with different possible modeling functions. The Fourier transform of the EXAFS functions was performed in the range  $1.97\text{--}13.76 \text{ \AA}^{-1}$ . The diminution of the Fourier transform magnitude arises as a result of the reduced average coordination number. From the evaluated values of the local structural parameters (Table 1), one can see that the coordination geometry of Fe sites in nanocrystallites (*nc*)  $\alpha\text{-Fe}_2\text{O}_3$  embedded in PPY differs significantly from that in the standard sample. EXAFS contains information about both surface and interior lattice disorder in *nc*  $\text{Fe}_2\text{O}_3$ . A more pronounced deviation from the crystalline structure of the standard sample could appear with the decrease of *nc* size. It could be due to the increase of the fraction of surface Fe sites that are substantially distorted [10]. The preedge peak of the absorption spectrum in the Figure 2 is more intense in the case of the 2PPY- $\text{Fe}_2\text{O}_3$  sample containing *nc*  $\text{Fe}_2\text{O}_3$  with smaller  $D_{\text{eff}}$  than that for the 1PPY- $\text{Fe}_2\text{O}_3$  sample.



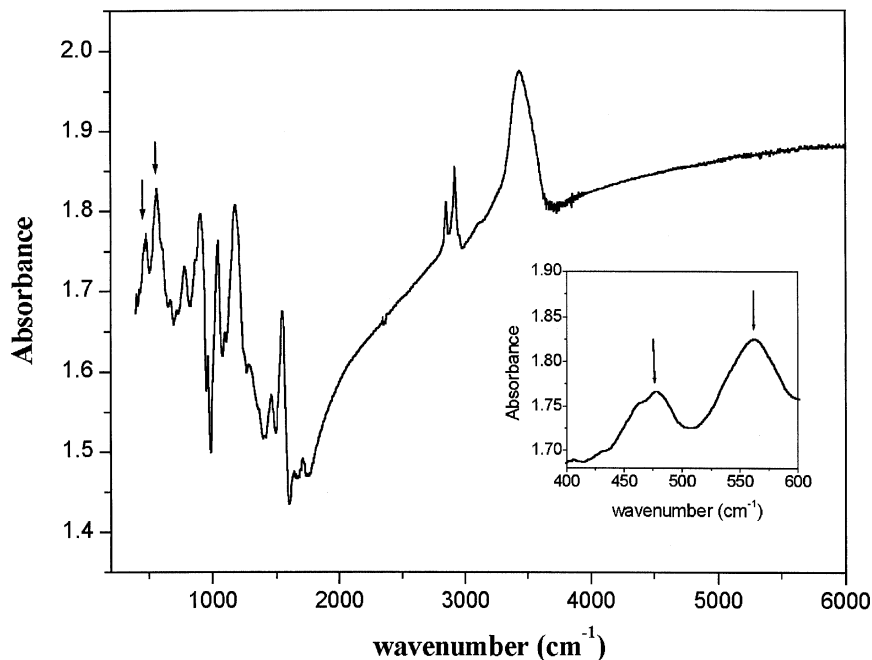
**FIGURE 2** EXAFS spectra for polypyrrole nanocomposites and for the standard  $\alpha\text{-Fe}_2\text{O}_3$ .

Figure 3 shows the FTIR absorption spectrum of the nanocomposite 2PPY- $\text{Fe}_2\text{O}_3$ . A similar spectrum was obtained for the sample 1PPY- $\text{Fe}_2\text{O}_3$ . One can identify the presence of the intense absorption bands located at  $905$ ,  $1040$ ,  $1175$  and  $1546\text{ cm}^{-1}$  which are characteristic for the vibrations of PPY [11]. This fact demonstrates that PPY matrix doesn't degrade during the successive chemical treatments with NaOH,  $\text{FeCl}_3$  and  $\text{NH}_4\text{OH}$ . The two intense bands located at  $560\text{ cm}^{-1}$  and  $470\text{ cm}^{-1}$ , which can be better observed in the inset of Figure 3, are characteristic for  $\alpha\text{-Fe}_2\text{O}_3$  [12].

Due to their small size, the *nc*  $\alpha\text{-Fe}_2\text{O}_3$  particles are not antiferromagnetically aligned and possess a small permanent magnetic moment due to the

**TABLE 1** The Local Structural Parameters of Fe Sites in  $\alpha\text{-Fe}_2\text{O}_3$  Crystallites Embedded in PPY and in a Standard Sample Respectively

Sample	Atomic number	Shell radius [ $\text{\AA}$ ]	Shift Energy [eV]
1PPY- $\text{Fe}_2\text{O}_3$	1.40	1.88	-3
2PPY- $\text{Fe}_2\text{O}_3$	1.42	1.92	2
$\alpha\text{-Fe}_2\text{O}_3$ standard	6	1.94	0



**FIGURE 3** FTIR spectrum for the nanocomposite 2PPY-Fe<sub>2</sub>O<sub>3</sub>.

imperfect compensation of magnetic sublattices. The magnetization,  $M$  of the investigated nanocomposites measured versus increasing and decreasing magnetic field shows no hysteresis loop (Fig. 4). This behavior is typical for nanosized magnetic particles, and it is consistent with a superparamagnetic behavior [1]. The best fit of the magnetization curve was obtained using the classical Langevin function with an additional term:

$$M = M_S \left[ \coth \left( \frac{mH}{k_B T} \right) - \frac{k_B T}{mH} \right] + \chi \cdot H \quad (3)$$

Here,  $M_S$  is the saturation magnetization,  $m$  is the average magnetic moment of the individual particle of Fe<sub>2</sub>O<sub>3</sub> in the sample and  $\chi \cdot H$  represents the contribution of the PPY matrix to the total magnetization. The following fitting parameters values were obtained:

Sample 1PPY-Fe<sub>2</sub>O<sub>3</sub> :  $M_S = 0.29$  emu/g,  $m/k_B T = 4.9 \times 10^{-3}$  G<sup>-1</sup>

and  $\chi = 2 \times 10^{-6}$  emu/g;

Sample 2PPY-Fe<sub>2</sub>O<sub>3</sub> :  $M_S = 0.46$  emu/g,  $m/k_B T = 3 \times 10^{-3}$  G<sup>-1</sup>

and  $\chi = 1.8 \times 10^{-6}$  emu/g



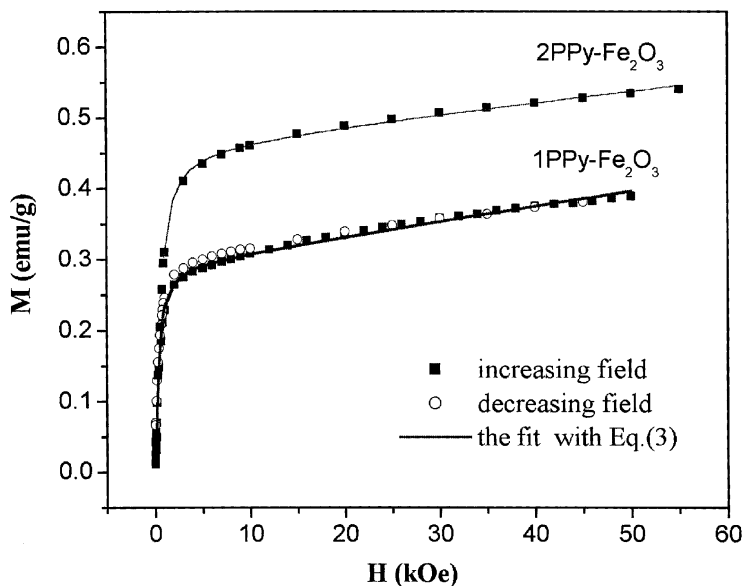


**FIGURE 4** The magnetization vs. applied magnetic field for polypyrrole nanocomposites at  $T = 300$  K.

By using the relation  $M_S = c \times m$  we have calculated the average specific concentrations of magnetic particles for the investigated nanocomposites:  $c_1 = 1.4 \times 10^{15} \text{ g}^{-1}$  and  $c_2 = 3.8 \times 10^{15} \text{ g}^{-1}$  for 1PPY- $\text{Fe}_2\text{O}_3$  and 2PPY- $\text{Fe}_2\text{O}_3$ , respectively. A higher concentration of  $\text{Fe}_2\text{O}_3$  nanoparticles is obtained for the sample 2PPY- $\text{Fe}_2\text{O}_3$  and consequently the specific saturation magnetization is higher for this sample than for 1PPY- $\text{Fe}_2\text{O}_3$ . This result shows that the most important step in the formation of the nanocomposite is the insertion of a high concentration of  $\text{Fe}^{3+}$  ions into the host PPY matrix and the diminution of polymer chains oxidation process by these ions.

The ESR spectra at room temperature for the investigated samples are shown in the Figure 5. Two resonance lines were identified: a narrow line and a broad one which can be attributed to the paramagnetic PPY matrix and the superparamagnetic  $\text{Fe}_2\text{O}_3$  nanoparticles respectively. The line shapes were found to be Lorentzian independently of the particle size. In order to evaluate the ESR parameters, the derivative spectra were fitted with a Lorentzian line shape, the fit parameters being the half-width at half-height,  $\Delta H_{1/2}$  of the corresponding absorption line and the resonance field  $H_0$ . The following values for  $g$ -factors and  $\Delta H_{1/2}$  were obtained:

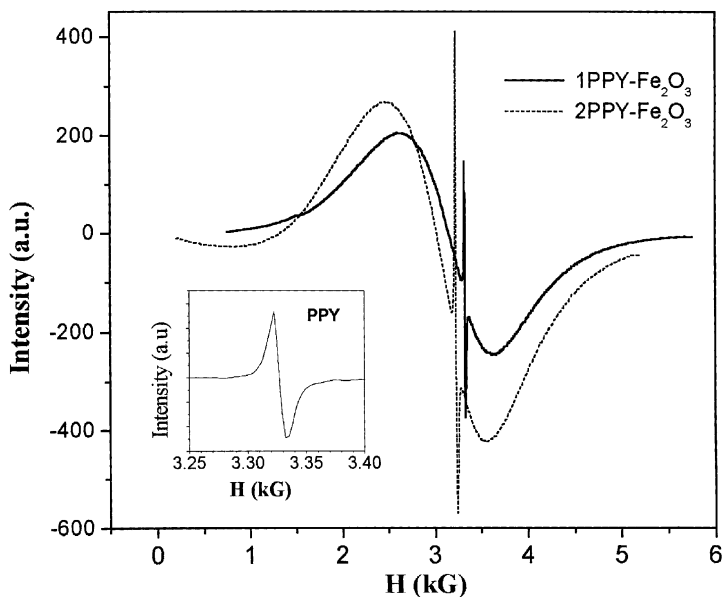


**FIGURE 5** ESR spectra for polypyrrole nanocomposites at  $T = 300$  K. Inset: ESR spectrum for PPY matrix with  $\Delta H_{1/2} = 13$  G.

PPY matrix :  $g = 2.0198, \Delta H_{1/2} = 13$  G;

$\text{Fe}_2\text{O}_3$  with  $D_{\text{eff}} = 67.77$  nm (sample 1PPY- $\text{Fe}_2\text{O}_3$ ):  $g = 2.133$ ,

$\Delta H_{1/2} = 1546$  G;

$\text{Fe}_2\text{O}_3$  with  $D_{\text{eff}} = 11.75$  nm (sample 2PPY- $\text{Fe}_2\text{O}_3$ ):  $g = 2.216$ ,

$\Delta H_{1/2} = 1619$  G.

The evaluated line widths decrease with the increase of the particle size. Our results are in agreement with that obtained by C.T. Hsieh *et al.* for  $\text{Fe}_2\text{O}_3$  nanoparticles prepared by sol-gel method [13]. This behavior could be attributed to the exchange narrowing mechanism, which become stronger as the particles size increase.

## CONCLUSIONS

The reported results represent the first steps concerning the synthesis and characterization of a new type of nanostructured composite with improved processability and low cost, obtained by the combination of a conducting polymer, PPY and  $\text{Fe}_2\text{O}_3$  nanoparticles.

XRD studies demonstrate the formation of *nc*  $\alpha$ -Fe<sub>2</sub>O<sub>3</sub> into the host PPY matrix. EXAFS investigation show that the coordination geometry of Fe sites in *nc*  $\alpha$ -Fe<sub>2</sub>O<sub>3</sub> embedded in PPY differs significantly from that in a standard polycrystalline  $\alpha$ -Fe<sub>2</sub>O<sub>3</sub>. Due to their small size and the presence of the structural distortion, the  $\alpha$ -Fe<sub>2</sub>O<sub>3</sub> nanoparticles embedded in PPY are not antiferromagnetic and exhibit a superparamagnetic behavior. A stronger magnetic exchange interaction in particles with larger size results in a narrower ESR line.

## REFERENCES

- [1] Kryszewski, M. & Jeszka, J. K. (1998). Nanostructured conducting polymer composites – superparamagnetic particles in conducting polymers. *Synthetic Metals*, 94, 99–104.
- [2] Gangopadhyay, R. & De, A. (1999). Polypyrrole-ferric oxide conducting nanocomposites I. Synthesis and characterization. *European Polymer Journal*, 35, 1985–1992.
- [3] Jing Liu & Meixiang Wan (2000). Composites of Polypyrrole with Conducting and Ferromagnetic Behaviors. *Journal of Polymer Science: Part A: Polymer Chemistry*, 38, 2734–2739.
- [4] Aldea, N. & Indrea, E. (1990). Fourier analysis of EXAFS data, a self contained FORTRAN program-package; the third version. *Comput. Phys. Commun.*, 60, 145–154.
- [5] San-Miguel, A. (1995). A program for fast classic or dispersive XAS data analysis in a PC. *Physica B*, 208/209, 177–179.
- [6] Resel, R., Turcu, R., Brie, M., Coldea, A., & Leising, G. (1999). Anisotropic properties of electrochemically grown polypyrrole films. *Romanian Reports in Physics*, 51, 695–703.
- [7] Aldea, N., Gluhoi, A., Marginean, P., Cosma, C., & Xie Yaning. (2000). Extended X-ray absorption fine structure and X-ray diffraction studies on supported nickel catalysts. *Spectrochimica Acta A, Part B*, 455, 997–1008.
- [8] Quadri, S. B., Yang, J. P., Skelton, E. F., & Ratna, B. R. (1997). Evidence if strain and lattice distortion in lead sulfide nanocrystallites. *Appl. Phys. Lett.*, 70, 1020–1021.
- [9] Klung, H. P. & Alexander, L. E. (1974). *X-ray diffraction procedures for polycrystalline and amorphous materials*. 2nd ed. John Wiley: New York, 662.
- [10] Chen, L. X., Liu, T., Thurnauer, Marion, C., Csencsits, R., Rajh, T. (2002). Fe<sub>2</sub>O<sub>3</sub> nanoparticle structures investigated by X-ray absorption near-edge structure, surface modifications and model calculations. *J. Phys. Chem. B*, 106, 8539–8546.
- [11] Turcu, R., Graupner, W., Filip, C., Bot, A., Brie, M., & Grecu, R. (1999). Studies of the intermolecular interactions in polypyrrole and conjugated composites based on polypyrrole. *Adv. Mater. Opt. Electron*, 9, 157–165.
- [12] Bentley, F. F., Smithson, L. D., Rozek, A. L. (1968). Infrared spectra and characteristic frequencies  $\sim 700\text{--}300\text{ cm}^{-1}$ . Interscience Publishers, John Wiley & Sons: New York.
- [13] Hseih, C. T., Huang, W. L., & Lue, J. T. (2002). The change from paramagnetic resonance to ferromagnetic resonance for iron nanoparticles made by the sol-gel method. *J. Phys. Chem. Solids*, 63, 733–741.